# p53 Translocation to Mitochondria Precedes Its Nuclear Translocation and Targets Mitochondrial Oxidative Defense Protein-Manganese Superoxide Dismutase

Yunfeng Zhao,[1] Luksana Chaiswing,[2,3] Joyce M. Velez,[1] Ines Batinic-Haberle,[4] Nancy H. Colburn,[5] Terry D. Oberley,[2,3] and Daret K. St. Clair[1]

[1]Graduate Center for Toxicology, University of Kentucky, Lexington, Kentucky; [2]Department of Pathology and [3]Veterans Affairs Medical Center, University of Wisconsin, Madison, Wisconsin; [4]Department of Radiation Oncology, Duke University, Durham, North Carolina; and [5]Gene Regulation Section, National Cancer Institute, Frederick, Maryland

## Abstract

**The tumor suppressor gene *p53* is activated by reactive oxygen species–generating agents. After activation, p53 migrates to mitochondria and nucleus, a response that eventually leads to apoptosis, but how the two events are related is unknown. Herein, we show that p53 translocation to mitochondria precedes its translocation to nucleus in JB6 skin epidermal cells treated with the tumor promoter 12-*O*-tetradecanoylphorbol-13-acetate (TPA). Translocation of p53 to mitochondria occurs within 10 minutes after TPA application. In the mitochondria, p53 interacts with the primary antioxidant enzyme, manganese superoxide dismutase (MnSOD), consistent with the reduction of its superoxide scavenging activity, and a subsequent decrease of mitochondrial membrane potential. In contrast to the immediate action on mitochondria, p53 transcriptional activity in the nucleus increases at 1 hour following TPA application, accompanied by an increase in the levels of its target gene *bax* at 15 hours following TPA treatment. Activation of p53 transcriptional activity is preventable by application of a SOD mimetic (MnTE-2-PyP$^{5+}$). Thus, p53 translocation to mitochondria and subsequent inactivation of MnSOD explains the observed mitochondrial dysfunction, which leads to transcription-dependent mechanisms of p53-induced apoptosis.** (Cancer Res 2005; 65(9): 3745-50)

## Introduction

Redox, or reduction/oxidation reaction, which involves the transfer of electrons or hydrogen atoms from one atom or molecule to another, is the major source of superoxide production from oxygen utilization. Superoxide radicals, the product of one electron reduction of molecular oxygen, are produced in the mitochondria as a result of the imperfect flow of electrons through the electron transport chain. At least two sites in the electron transport chain, complex I and ubisemiquinone, have been identified as primary sources of superoxide production in mitochondria (1, 2). Although superoxide radicals are not considered highly reactive compared with other reactive oxygen species, their toxicity may, in part, be due to their strategic location in the mitochondria and their effectiveness in striking critical targets in the respiratory chain. Thus, it is not surprising that manganese superoxide dismutase (MnSOD), the enzyme defending against superoxide radicals in the mitochondrial matrix, is essential for the survival of aerobic life (3). MnSOD homozygous knockout mice are small at birth and die within 2 to 3 weeks from dilated cardiomyopathy and neurodegenerative disease (4, 5). MnSOD knockout mice that live longer than 1 week exhibit extensive mitochondrial injury with degeneration of neurons and cardiomyocytes (5).

The p53 tumor suppressor, a homotetrametric transcription factor induced by DNA-damaging and oxidative stress–generating agents, has been called the guardian of the genome (6). Activation of apoptosis is an important mechanism in p53 tumor suppression. Apoptosis mediated by p53-dependent transcriptional activation of its target genes has been extensively studied (7, 8). However, evidence linking p53-induced apoptosis to oxidative stress and mitochondria has recently received considerable attention. First, p53-mediated apoptosis was preceded by activation of various oxidoreductases and reactive oxygen species generation before mitochondrial perturbation (9). Second, p53 activates the transcription of several mitochondrial proapoptotic proteins including Bax, a proapoptotic member of the Bcl-2 family (10); Noxa, a BH3-only member of the Bcl-2 family (11); and p53AIP1, a p53-regulated apoptosis inducing protein-1 (12). Third, a fraction of p53 is localized in the mitochondria at the onset of p53-dependent apoptosis preceding changes in mitochondrial membrane potential, cytochrome *c* release, and caspase activation (13–15). Thus, it has been suggested that p53 may mediate apoptosis by mechanisms that are both dependent and independent of its transcriptional activity, thereby amplifying its apoptosis potency.

Our previous studies showed that overexpression of human MnSOD reduced tumorigenicity in a multistage skin carcinogenesis mouse model (16). However, in a heterozygous MnSOD-knockout skin carcinogenesis model, the incidence and multiplicity of papillomas were similar in wild-type mice and MnSOD-deficient mice, although the levels of several oncoproteins and cell mitosis were increased to a higher degree than that in control wild-type epidermis (17). Biochemical and quantitative immunogold ultrastructural studies of mouse epidermis revealed increased frequency of apoptosis and activation of p53 in the MnSOD-deficient mice. Interestingly, we observed an increase in mitochondrial p53 immunoreactive protein levels that was much greater than the increase measured in the nucleus, suggesting that p53 translocation to mitochondria might contribute to mitochondria-initiated apoptosis.

In this report, we extend our previous studies on p53 activation during early stages of the skin carcinogenesis model to investigate the link between mitochondrial p53 and nuclear p53 during oxidative stress–induced apoptosis. Our current results show that treatment of skin epidermal JB6 cells (18) in culture with the tumor

**Requests for reprints:** Daret St. Clair, Graduate Center for Toxicology, University of Kentucky, Lexington, KY 40536. Phone: 859-257-3956; Fax: 859-323-1059; E-mail: dstcl00@pop.uky.edu.

promoter 12-*O*-tetradecanoylphorbol-13-acetate (TPA) resulted in p53 translocation to mitochondria, and this movement of p53 to mitochondria precedes its action in the nucleus. Furthermore, mitochondrial p53 targets MnSOD and inhibits its superoxide scavenging activity, resulting in modulation of p53 transcriptional activity. These results show a novel role of p53 in the mitochondria and link the effects of p53 in the mitochondria to its proapoptotic transcriptional effects in the nucleus.

## Materials and Methods

**Cell line and 12-*O*-tetradecanoylphorbol-13-acetate treatment.** JB6 $P^+$ (Cl 41, promotable by TPA treatment) was established and maintained as previously described (18). The cells were grown in EMEM medium supplemented with 4% fetal bovine serum, 2 mmol/L of L-glutamine, 50 μg/mL penicillin, and 50 μg/mL streptomycin. TPA (1 mmol/L, Sigma, St. Louis, MO) stock solution in DMSO was prepared. It was diluted in culture medium to a final concentration of 100 nmol/L for treatment of cells. DMSO (0.01%) diluted in medium was used as vehicle control.

**Detection of mitochondrial membrane potential.** Five thousand JB6 cells were seeded in 96-well plates with 150-μL medium. Twenty-four hours after plating, the cells were treated with TPA (100 nmol/L) for 5 minutes to 4 hours. After washing with cold PBS (pH 7.4) and incubating in culture medium containing 2 μg/mL of JC-1 for 30 minutes, the dye was removed and cells were washed with PBS. Fluorescence intensity was measured immediately by fluorescence spectrometry (Spectra MAX GEMINI, Molecular Devices, Sunnyvale, CA). For JC-1 green, $E_x$ = 485 and $E_m$ = 525; for JC-1 red, $E_x$ = 535 and $E_m$ = 590.

**Fluorescent staining of p53 immmunoreactive protein.** Ten thousand JB6 cells were seeded in 8-well Lab-Tek Chamber Slides w/Cover (Nalge Nunc International, Naperville, IL) in 400-μL medium and incubated overnight. Twenty-four hours after plating, cells were incubated with 200 nmol/L of MitoTracker Red CMXRos (Molecular Probes, Eugene, OR) in culture medium for 30 minutes, after which the dye was removed, and cells were treated with TPA (100 nmol/L) for 5 minutes to 4 hours. Cells were washed and fixed in 2% formaldehyde containing 0.1% glutaraldehyde for 15 minutes at room temperature. After rinsing with cold PBS (pH 7.4), cells were permeabilized with 0.5% Triton X-100 for 10 minutes at room temperature. After blocking, anti-p53 antibody (Ab-11, Oncogene, Boston, MA) was added (1:64 dilution) and incubated at 37°C for 1 hour followed by incubation with anti-mouse IgG-FITC (Sigma, 1:128 dilution) for 1 hour. After removal of antibodies, the cells were rinsed with PBS and mounted with 90% glycerol.

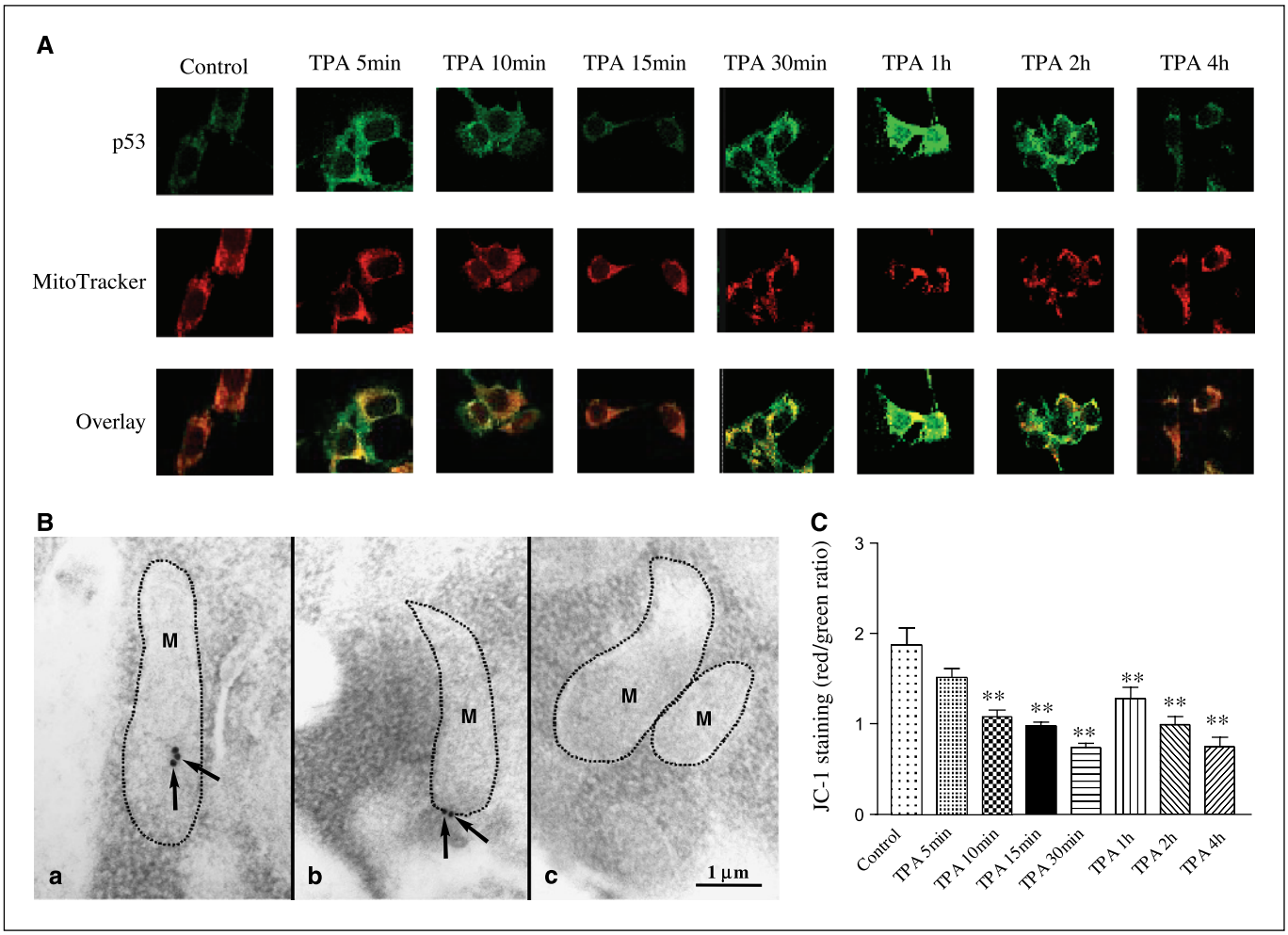


**Figure 1.** p53 rapid translocation into mitochondria and subsequent decreases in mitochondrial membrane potential. *A,* immunofluorescence staining of p53 in mitochondria. *Green,* p53 staining; *red,* MitoTracker Red as mitochondrial marker. *B,* electron microscopic examination of p53 in the mitochondria using immunogold labeling. After treatment with TPA for 1 hour, JB6 cells showed that p53 was located in the matrix (*a*, *arrows*) and at the outer membrane of mitochondria (*b*, *arrows*). In vehicle control-treated cells, there was no p53 staining (*c*). *M,* mitochondria. *C,* detection of mitochondrial membrane potential using JC-1 staining. The ratio of aggregates (fluorescence intensities at 590 nm) and monomer (fluorescence intensities at 525 nm) was plotted as an indicator of mitochondrial membrane polarization. *Columns,* means of four independent experiments; *bars,* SE. Statistical analysis was done using one-way ANOVA followed by Newman-Keuls post-test. **, $P < 0.01$ when compared with *control* (no treatment).

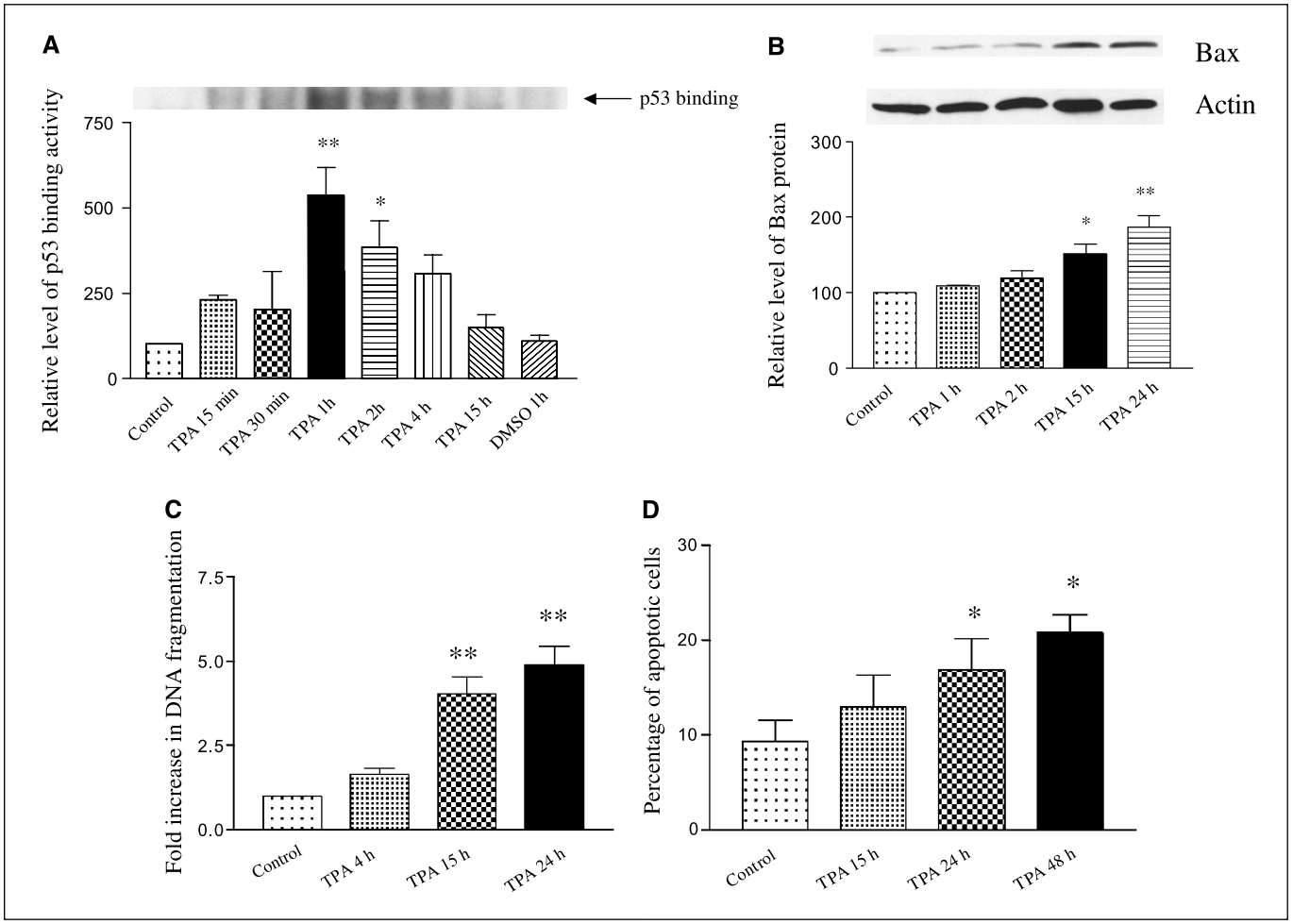


**Figure 2.** Transcriptional activation of p53 and apoptosis following TPA treatment. JB6 cells were grown in P100 plates and TPA was added when cells reached 70% confluence. *A,* EMSA analysis of p53-DNA binding. *Columns,* means of three independent experiments; *bars,* SE EMSA. One representative result. *B,* quantitation of Bax protein. *Columns,* means of four independent experiments; *bars,* SE Western blot. One representative result. *C,* quantitation of DNA fragmentation using cell death ELISA analysis. *Columns,* means of four independent experiments; *bars,* SE. *D,* quantitation of apoptotic cell population detected by Hoechst/merocyanine 540 staining. *Columns,* means of four independent experiments; *bars,* SE. Statistical analysis was one-way ANOVA followed by Newman-Keuls post-test. *, $P < 0.05$ when compared with *control* (no treatment). **, $P < 0.01$ when compared with *control*.

Fluorescence was immediately observed using a Leica laser scanning confocal microscope (Bensheim, Germany; magnification, 64×).

For studies on the suppression of nuclear translocation of p53 by a SOD mimetic (MnTE-2-PyP$^{5+}$, Mn[III] tetrakis[*N*-ethylpyridinium-2-yl]porphyrin), JB6 cells were treated with 100 nmol/L TPA for 10 minutes followed by an addition of 80 pg/mL MnTE-2-PyP$^{5+}$ for 50 minutes. After staining with p53 immunoreactive protein following the steps described above, cells were stained with 50 μg/mL of Hoechst 33342 for 10 minutes before being observed under confocal microscopy (magnification, 64×).

**Immunogold labeling of p53 protein in mitochondria.** After treatment with TPA (100 nmol/L) for 1 hour, JB6 cells were fixed for 1 hour in Carson Millonig's fixative followed by rinsing with 0.1 mol/L Sorenson's phosphate buffer for 30 minutes. Cells were dehydrated in graded ethanol and embedded in LR White resin. LR white embedded blocks were trimmed and sectioned. Thin sections were mounted on 1% collodion membrane–coated nickel grids. Sections were rinsed with TBS and treated with bovine serum albumin-C blocking solution (Aurion, AA Wageningen, the Netherlands) for 30 minutes to block nonspecific staining and then washed with TBS for 5 minutes. The grids were incubated with primary antibody at 4°C overnight. After incubation, grids were rinsed in four changes of TBS washing buffer for 5 minutes each and one change of alkaline TBS for 10 minutes. Grids were incubated with gold (15 nm)–conjugated secondary antibody (Amersham, Piscataway, NJ; diluted at 1:75) for 90 minutes at room temperature. Grids were washed and counterstained with 2% uranyl acetate (10 minutes), and observed and photographed with a Hitachi H-600 electron microscope (Schaumburg, IL; amplification, 21,600×). As a control, normal serum was used in place of primary antibody.

**Isolation of mitochondrial fraction from JB6 cells.** After treatment with vehicle (0.01% DMSO) for 1 hour or TPA (100 nmol/L) for 1 or 24 hours, cells were suspended in 2 mL mitochondria isolation buffer [0.225 mol/L mannitol, 0.075 mol/L sucrose, 1 mmol/L EGTA (pH adjusted to 7.4 with a few drops of 0.5 mol/L Tris)] in a 10-mL Wheaton homogenizer tube and carefully homogenized for 30 strokes on ice. The cell debris was removed by centrifugation at 576 × *g* (2,200 rpm) for 5 minutes in a Sorval SS34 rotor. The supernatant was filtered through a nylon screen cloth (Small Parts, Inc., Miami Lakes, FL) and centrifuged at 9,000 × *g* (8,700 rpm) for 10 minutes. The pellet was washed by adding 0.5 mL of mitochondria isolation buffer and centrifuging at 9,000 × *g* for 5 minutes. This washing step was done twice. The mitochondrial pellet was resuspended in 300 μL of mitochondria isolation buffer containing 0.1% Triton X-100 and protease inhibitors (5 μg/mL of pepstatin, leupeptin, and aprotinin). This fraction was labeled as the *mitochondria fraction* and kept at −80°C.

**Immunoprecipitation.** Anti-MnSOD antibody (Upstate, Charlottesville, VA) or anti-p53 antibody was crossed-linked to protein A/G-agarose beads (Life Technologies, Carlsbad, CA) using disuccinimidyl suberate according to the instructions provided by the manufacturer (Pierce, Rockford, IL). Five

hundred micrograms of the mitochondrial fraction from JB6 cells treated with DMSO/TPA or 200 μg of the mitochondrial fraction from C57BL/6 MnSOD deficient mouse skin epidermis originally treated *in vivo* with a single dose of 100 nmol/L 7,12-dimethylbenz(a)anthracene (DMBA) followed by a single application of 4 μg TPA for 24 hours (17) were incubated with the antibody-agarose bead conjugate in PIRA buffer [PBS (pH 7.4), containing 1% NP40, 0.5% sodium deoxycholate, and 0.1% SDS] at 4°C overnight. After washing five times with PIRA buffer, the immunoprecipitated proteins were eluted thrice with 100 μL of 50 mmol/L Tris-glycine buffer (pH 2.4). The eluates were collected separately and immediately analyzed by Western blotting.

**MnSOD activity assay.** The same mitochondrial fraction used for immunoprecipitation was frozen and thawed thrice. The resulting lysate was used for MnSOD activity assay by the nitroblue tetrazonium-bathocuproinedisulfonic acid reduction inhibition method as described by Spitz and Oberley (19). The protein level of MnSOD was detected by Western blots and densitometry.

**Preparation of nuclear extract.** Cells were collected and suspended in 400 μL of buffer A [10 mmol/L HEPES-KOH with 1.5 mmol/L $MgCl_2$, 10 mmol/L KCl, 0.2 mmol/L phenylmethylsulfonyl fluoride (PMSF), 5 μmol/L of DTT, and protease inhibitors]. The samples were kept on ice for 15 minutes, 12.5 μL of 10% NP40 were added, and the samples were vortexed vigorously for 15 seconds. The lysate was centrifuged at 14,000 rpm (or 17,500 × *g*) for 30 seconds. The pellet was dissolved in 100 μL of buffer B [20 mmol/L HEPES/KOH with 1.5 mmol/L $MgCl_2$, 420 mmol/L NaCl, 35% glycerol, 0.2 mmol/L PMSF, 5 μmol/L DTT, 0.2 mmol/L EDTA (pH 8.0), and protease inhibitors] and kept on ice for 20 minutes followed by centrifugation at 12,000 rpm for 2 minutes. The supernatant, identified as the *nuclear extract*, was frozen at −80°C.

**Electrophoretic mobility shift assays.** p53-DNA binding activity was analyzed using the nuclear extract fraction. The p53 double-stranded oligonucleotide (5′-TACAGAACATGTCTAAGCATGCTGGGG-3′) was purchased from Santa Cruz Biotechnology (Santa Cruz, CA). A 25-μL reaction solution containing 6 μg of the nuclear extract, 5 μL of 5× binding buffer [50 mmol/L Tris-HCl (pH 7.4), with 20% glycerol, 5 mmol/L $MgCl_2$, 2.5 mmol/L EDTA, 5 mmol/L DTT, and 0.25 mg/mL poly dI-dC] and 0.4 μg of anti-p53 antibody (Ab-11, Oncogene), was incubated for 1 hour at room temperature. Then a 50,000-cpm labeled probe was added and incubated at room temperature for 20 minutes. Three microliters of 10× loading buffer were added, and samples were separated on a 6% native polyacrylamide gel for 3 to 4 hours. DNA-protein complexes were visualized by exposing the gels to Kodak film at −80°C.

**Detection of apoptosis by flow cytometry.** After treatment with TPA (100 nmol/L) for 15, 24, and 48 hours, cells were washed with cold PBS (pH 7.4) and removed from culture dishes using Cell Dissociation Solution (Sigma) and passed through a nylon screen cloth (Small Parts) to obtain a single cell suspension. Combined Hoechst 33342 (Molecular Probes) and merocyanine 540 (Molecular Probes) staining was used to distinguish the apoptotic cell population (20).

**Nucleosome fragmentation assay.** DNA fragmentation was detected by cell death detection ELISA (Roche, Indianapolis, IN) according to the manufacturer's instructions with minor modifications: after treatment with 100 nmol/L TPA, cells were collected and lysed and 25 μL of the whole cell lysate were applied to each sample well.

**Western blot analysis.** For detection of the protein levels of Bax or MnSOD, 20 μg of the whole cell lysate or mitochondrial fraction were separated on 10% SDS-PAGE gels and transferred to a nitrocellulose membrane. Ponceau staining was used to monitor the uniformity of transfer. The membrane was blocked in Blotto [5% milk, 10 mmol/L Tris- HCl (pH 8.0), 150 mmol/L NaCl, and 0.05% Tween 20] for 2 hours at room temperature. Anti-Bax antibody (Santa Cruz Biotechnology, 1:1,000 dilution) or anti-MnSOD antibody (Upstate, 1:2,000 dilution) was added and incubated for 2 hours at room temperature. After washing, the membrane was incubated with horseradish peroxidase–conjugated secondary antibodies (Santa Cruz Biotechnology) at a 1:4,000 dilution. The antibody bands were visualized by the enhanced chemiluminescence detection system (Amersham). The membranes were then stripped and reprobed with a monoclonal anti-actin antibody (Sigma, 1:2,000 dilution) or anti-mitochondrial HSP70 (ABR-Affinity BioReagents, Golden, CO; 1:2,000 dilution), respectively, to normalize protein loading. The corresponding bands were scanned, and the densities were quantitatively assessed using imageQuant 5.1 software (Bio-Rad, Hercules, CA).

**Statistical analysis.** Statistical analysis was done using either Student's *t* test (for two-group comparison) or one-way ANOVA (for multiple-group comparison) followed by Newman-Keuls post-test. Data are reported as means ± SE.

## Results

We have previously observed an increase in the levels of both mitochondrial p53 and nuclear p53 in a multistage skin carcinogenesis model (17). Following TPA treatment of skin epidermal JB6 cells, p53 translocated to both mitochondria and nucleus as monitored by immunofluorescence staining of immunoreactive p53 protein (Fig. 1*A*). p53 was then increased in the mitochondria as early as 5 and 10 minutes after application of TPA, shown by its colocalization with the mitochondrial marker MitoTracker (red fluorescence). At 1 hour following TPA treatment, the green fluorescence was detected in both mitochondria and nucleus, which indicated that translocation of p53 to mitochondria preceded its translocation to nuclei. The nuclear p53 was decreased at 2 hours and reduced to control level at 4 hours after TPA treatment.

p53 translocation to the mitochondria was further verified by immunogold labeling of JB6 cells 1 hour after TPA treatment, when the most intensive p53 staining was observed in the mitochondria. As shown in Fig. 1*B*, p53 was found in the mitochondrial matrix (*a*, *arrows*) and at the outer membrane of mitochondria (*b*, *arrows*) but was not detectable in the mitochondria of vehicle-treated cells (*c*).

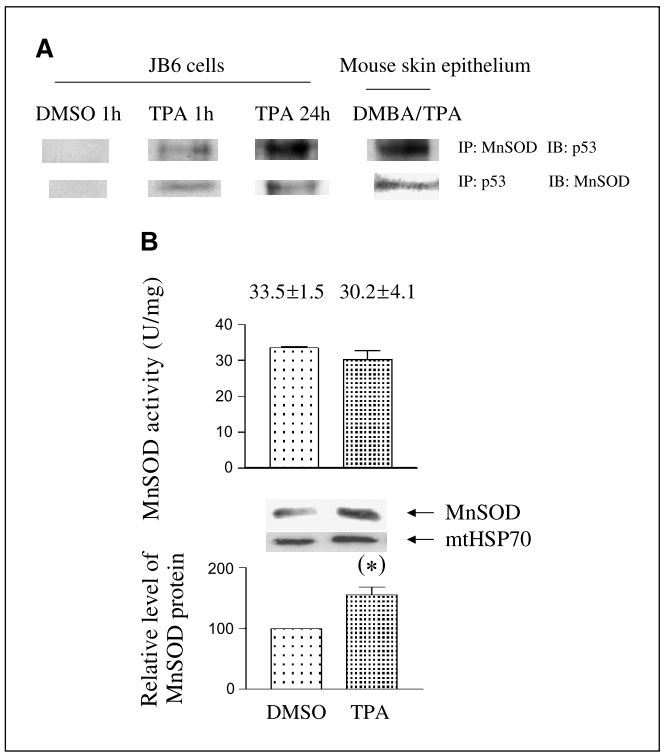


**Figure 3.** p53 interaction with MnSOD. *A,* immunoprecipitation of p53 or MnSOD with anti-MnSOD or anti-p53 antibody. *B,* inhibition of MnSOD activity. *Columns,* means of three independent experiments; *bars,* SE Western blot. One representative result. *Top,* MnSOD activity measured by NBT-BCS reduction inhibition assay. *Bottom,* quantitation of MnSOD protein from Western blot. Statistical analysis was done using Student's *t* test. *, $P < 0.05$ when compared with vehicle.

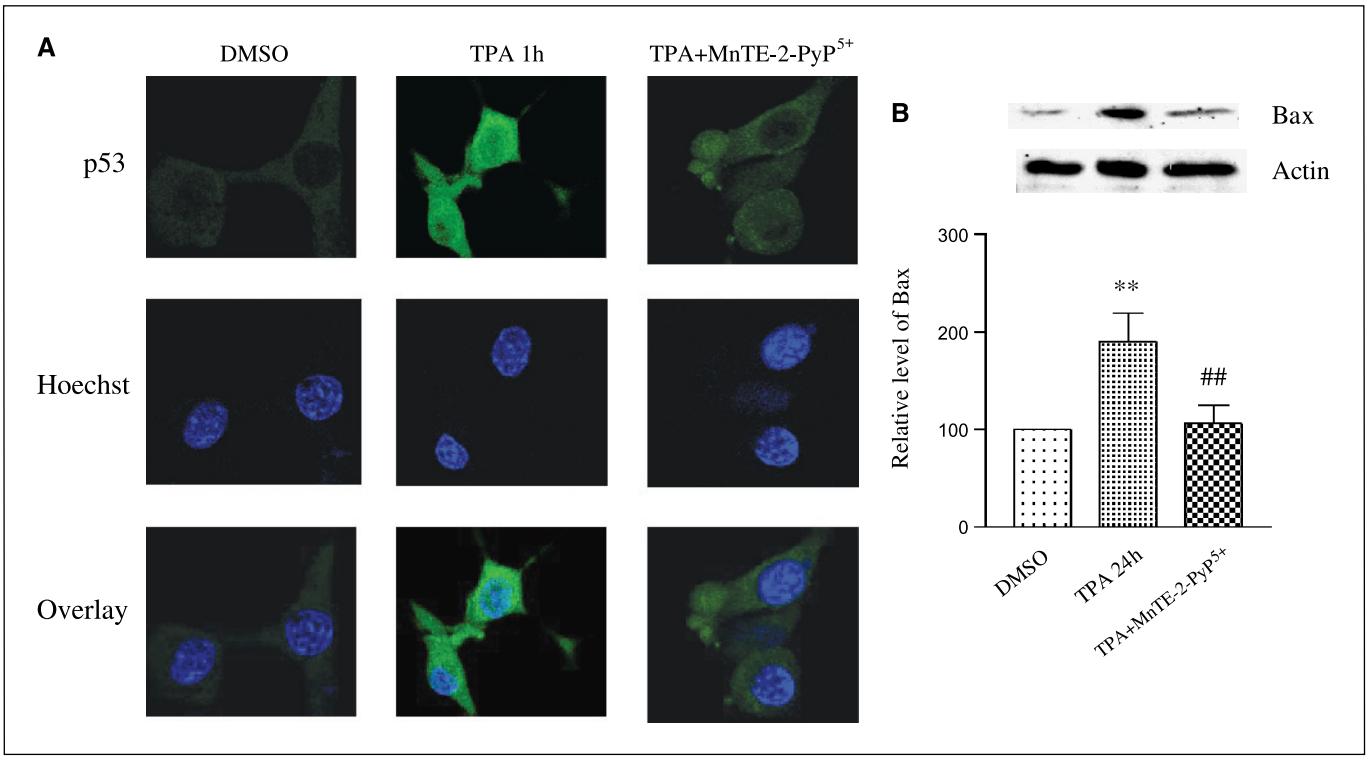


**Figure 4.** *A,* immunofluorescence staining of p53 in the nucleus after treatment with a SOD mimetic (MnTE-2-PyP$^{5+}$). TPA (100 nmol/L) was applied 10 minutes before addition of MnTE-2-PyP$^{5+}$ (80 pg/mL). *Green,* p53 staining; *blue,* Hoechst 33342 staining. *B,* MnTE-2-PyP$^{5+}$ suppression of the induction of Bax. *Columns,* means of four independent experiments; *bars,* SE Western blot. One representative result. Statistical analysis was done using one-way ANOVA followed by Newman-Keuls post-test. **, $P < 0.01$ when compared with vehicle control. ##, $P < 0.01$ when compared with TPA treatment.

We observed decreased mitochondrial membrane potential following p53 translocation into mitochondria as detected by JC-1 (5′,5′,6,6′-tetrachloro-1,1′,3,3′-tetraethyl-benzimidazolylcarbocyanine iodide) staining. JC-1 is a ratiometric dye that forms aggregates in a membrane potential-dependent fashion. The ratio of aggregates [fluorescence intensities at 590 nm (red)] and monomers [fluorescence intensities at 525 nm (green)] reflects the level of mitochondrial membrane polarization. As shown in Fig. 1*C*, the red/green fluorescence ratio began to decrease by 5 minutes, reached a minimum level by 30 minutes, and remained at low levels throughout the remainder of the time points examined.

The DNA binding activity of p53 was measured by electrophoretic mobility shift assays (EMSA) and the results were quantified and summarized in Fig. 2*A*. A maximum DNA binding activity occurred at 1 hour after TPA treatment, which is consistent with its nuclear translocation. To further verify the transcriptional effect of p53, the protein levels of *Bax*, a p53 target gene and a member of the proapoptotic Bcl-2 family, were analyzed. The quantified results were shown in Fig. 2*B*. The protein levels of Bax increased with time and reached a significant level by 15 hours after TPA treatment.

The observed increase in p53 activation was associated with an increase in nuclear DNA fragmentation detected by a nucleosome fragmentation assay (Fig. 2*C*). The increase of nuclear DNA fragmentation was consistent with the increase of Bax protein and reaching a significant level by 15 hours following TPA treatment. Apoptotic cell death was further confirmed using Hoechst/merocyanine 540 staining. As shown in Fig. 2*D*, percentage of apoptotic cells increased with time and reached a significant level at 24 and 48 hours following TPA treatment.

It has been shown that p53 could induce apoptosis independently of transcriptional activation of p53 target genes (21). Recent studies indicate that p53 binds to multiple targets in the mitochondria to exert its activity as an apoptosis inducer. These targets include p53AIP1 (12), Bcl-2/Bcl-$x_L$ (22), and Bax (23); all of which are located in the outer membrane of mitochondria. However, our ultrastructural results revealed that mitochondrial p53 localized to both the outer membrane and the matrix of mitochondria. Because the primary antioxidant defense protein, MnSOD, is located in the mitochondrial matrix, we postulated that it might be the target of matrix-localized p53. To determine whether p53 interacts with MnSOD in the mitochondria, we did immunoprecipitation using mitochondria isolated from both JB6 cells treated with either DMSO (vehicle control) or 100 nmol/L TPA for 1 or 24 hours. Mitochondria isolated from mouse skin tissues treated with a single application of DMBA (100 nmol/L) followed by a single dose (4 μg) of TPA for 24 hours were used to probe the interactions between p53 and MnSOD *in vivo*. As shown in Fig. 3*A*, p53 protein was detected in the mitochondria of both TPA-treated JB6 cells and mouse skin epidermis when the mitochondrial protein extracts were immunoprecipated with anti-MnSOD antibody but was undetectable in DMSO-treated mitochondrial extracts of JB6 cells. Vice versa, MnSOD protein was detected in the mitochondria of both TPA-treated JB6 cells and mouse skin epidermis when the mitochondrial protein extracts were immunoprecipated with anti-p53 antibody, suggesting physical interaction between p53 and MnSOD in the mitochondria.

We (24) and others (25) have shown that TPA can induce *MnSOD* gene transcription in many cell types. In light of the novel findings on the interaction between p53 and MnSOD and the potential for p53 to

inactivate MnSOD activity, we compared the levels of MnSOD activity with protein levels after TPA treatment. As shown in Fig. 3*B*, total MnSOD immunoreactive proteins was increased by 60% after TPA treatment; in contrast, the MnSOD superoxide scavenging activity was decreased by 11%, suggesting that p53 binding to MnSOD leads to an inhibition of MnSOD activity in the mitochondria.

To probe the possibility that inactivation of MnSOD with resultant oxidative stress may activate the translocation of p53 into the nucleus, we treated JB6 cells with TPA for 10 minutes to promote the observed early mitochondrial accumulation of p53; added a well-characterized SOD mimetic (26), MnTE-2-PyP$^{5+}$; and analyzed the nuclear translocation of p53. As shown in Fig. 4*A*, immunofluorescence staining showed that MnTE-2-PyP$^{5+}$ only slightly reduced the levels of mitochondrial p53 but completely blocked the translocation of p53 into the nucleus. Consistent with the lack of p53 accumulation in the nucleus, the level of Bax protein was not increased after TPA and MnTE-2-PyP$^{5+}$ cotreatment (Fig. 4*B*).

## Discussion

Our previous studies on the effects of MnSOD on tumorigenesis using the multistage skin carcinogenesis mouse model showed that treatment with TPA not only promoted cell proliferation but also induced apoptosis *in vivo* (17). We had also showed that activation of p53 was associated with apoptosis events *in vivo* (17). In addition, the levels of p53 were increased in both mitochondrial and nuclear compartments, suggesting that p53 translocation into mitochondria may also play a role in TPA-induced apoptosis during the promotion phase of skin tumorigenesis (17).

Increasing evidence supports the presence of p53 in mitochondria and suggests that mitochondrial p53 localization is sufficient for initiating p53-dependent apoptosis (14, 27). Furthermore, some studies suggest that p53 may induce apoptosis by forming complexes with mitochondrial proapoptotic proteins such as p53AIP1 (14) Bcl-2/Bcl-$x_L$ (22), all of which are located in the outer membrane of mitochondria. In this study, we showed that p53 translocated not only to the outer membrane of mitochondria but also into the matrix. Furthermore, p53 in the mitochondrial matrix interacted with the first layer of oxidative defense, MnSOD, leading to a reduction of MnSOD superoxide scavenging activity. These data highlight the role of redox balance in p53-induced apoptosis.

The present investigation shows the relationship between p53 translocation to mitochondria and p53-induced transcription of mitochondria-anchored proapoptotic genes, as indicated by the expression of Bax. Further studies will include other proapoptotic genes such as *Bak* and *p53AIP1*. Overall, this is the first study to show that mitochondrial p53 may play a direct role in the regulation of oxidative stress by interacting with MnSOD in the mitochondria and inhibiting MnSOD superoxide scavenging activity. The results also suggest that p53-mediated MnSOD inactivation in the mitochondria leads to the activation of p53 transcriptional function and subsequent induction of its proapoptotic target genes. The establishment of MnSOD as a target of p53 in the mitochondria reveals a novel strategy that could be exploited for either developing an antioxidant based cancer therapy or sensitizing cancer to radiation- or chemo-based therapies.

## Acknowledgments

Received 10/25/2004; revised 1/24/2005; accepted 2/18/2005.

**Grant support:** NIH grants CA 73599 and CA 49797; Thailand Research Fund under the Golden Jubilee Program (L. Chaiswing); and DOD CDMRP BC024326 (I. Batinic-Haberle).

The costs of publication of this article were defrayed in part by the payment of page charges. This article must therefore be hereby marked *advertisement* in accordance with 18 U.S.C. Section 1734 solely to indicate this fact.

We thank Mary Gail Engle and Mary Jennes at the University of Kentucky Imaging facility for their technical support on laser confocal experiments; Jennifer Strange and Greg Bauman for their technical support on fluorescence-activated cell sorting analysis; and the William S. Middleton Memorial Veterans Administration Hospital (Madison, WI) for resources and use of facilities.

## References

1. Chance B, Sies H, Boveris A. Hydroperoxide metabolism in mammalian organs. Physiol Rev 1979;59:527–605.
2. Halliwell B, Gutteridge JM. Oxygen free radicals and iron in relation to biology and medicine: some problems and concepts. Arch Biochem Biophys 1986;246:501–14.
3. Fridovich I. Superoxide radical and superoxide dismutases. Annu Rev Biochem 1995;64:97–112.
4. Li Y, Huang TT, Carlson EJ, et al. Dilated cardiomyopathy and neonatal lethality in mutant mice lacking manganese SOD. Nat Genet 1995;11:376–81.
5. Lebovitz RM, Zhang H, Vogel H, et al. Neurodegeneration, myocardial injury and perinatal death in mitochondrial superoxide dismutase-deficient mice. Proc Natl Acad Sci USA 1996;93:9782–7.
6. Lane DP. Cancer: p53, guardian of the genome. Nature 1992;358:15–6.
7. Tokino T, Nakamura Y. The role of p53-target genes in human cancer. Crit Rev Oncol Hematol 2000;33:1–6.
8. Moll UM, Zaika A. Nuclear and mitochondrial apoptotic pathways of p53. FEBS Lett 2001;493:65–9.
9. Polyak K, Xia Y, Zweier JL, Kinzler KW, Vogelstein B. A model for p53-induced apoptosis. Nature 1997;389:300–5.
10. Miyashita T, Reed JC. Tumor suppressor p53 is a direct transcriptional activator of the human bax gene. Cell 1995;80:293–9.
11. Oda E, Ohki R, Murasawa H, et al. Noxa, a BH3-only member of the Bcl-2 family and candidate mediator of p53-induced apoptosis. Science 2000;288:1053–8.
12. Oda K, Arakawa H, Tanaka T, et al. p53AIP1, a potential mediator of p53-dependent apoptosis, and its regulation by Ser-46-phosphorylated p53. Cell 2000;102:849–62.
13. Li PF, Dietz R, von Harsdorf R. p53 regulates mitochondrial membrane potential through reactive oxygen species and induces cytochrome *c*-independent apoptosis blocked by Bcl-2. EMBO J 1999;18:6027–36.
14. Marchenko ND, Zaika AI, Moll UM. Death signal-induced localization of p53 protein to mitochondria. A potential role in apoptotic signaling. J Biol Chem 2000;275:16202–12.
15. Erster S, Mihara M, Kim RH, Petrenko O, Moll UM. *In vivo* mitochondrial p53 translocation triggers a rapid first wave of cell death in response to DNA damage that can precede p53 target gene activation. Mol Cell Biol 2004;24:6728–41.
16. Zhao Y, Xue Y, Oberley TD, et al. Overexpression of manganese superoxide dismutase suppresses tumor formation by modulation of activator protein-1 signaling in a multistage skin carcinogenesis model. Cancer Res 2001;61:6082–8.
17. Zhao Y, Oberley TD, Chaiswing L, et al. Manganese superoxide dismutase deficiency enhances cell turnover via tumor promoter-induced alterations in AP-1 and p53-mediated pathways in a skin cancer model. Oncogene 2002;21:3836–46.
18. Colburn NH, Former BF, Nelson KA, Yuspa SH. Tumour promoter induces anchorage independence irreversibly. Nature 1979;281:589–91.
19. Spitz DR, Oberley LW. An assay for superoxide dismutase activity in mammalian tissue homogenates. Anal Biochem 1989;195:133–40.
20. Reid S, Cross R, Snow EC. Combined Hoechst 33342 and merocyanine 540 staining to examine murine B cell cycle stage, viability and apoptosis. J Immunol Methods 1996;192:43–54.
21. Caelles C, Helmberg A, Karin M. p53-dependent apoptosis in the absence of transcriptional activation of p53-target genes. Nature 1994;370:220–3.
22. Mihara M, Erster S, Zaika A, et al. p53 has a direct apoptogenic role at the mitochondria. Mol Cell 2003;11:577–90.
23. Chipuk JE, Kuwana T, Bouchier-Hayes L, et al. Direct activation of Bax by p53 mediates mitochondrial membrane permeabilization and apoptosis. Science 2004;303:1010–4.
24. Porntadavity S, Xu Y, Kiningham K, et al. TPA-activated transcription of the human *MnSOD* gene: role of transcription factors SP-1 and Egr-1. DNA Cell Biol 2001;20:473–81.
25. Fujii J, Taniguchi N. Phorbol ester induces manganese-superoxide dismutase in tumor necrosis factor-resistant cells. J Biol Chem 1991;266:23142–6.
26. Batinic-Haberle I, Spasojevic I, Hambright P, Benov L, Crumbliss AL, Fridovich I. Relationship among redox potentials, proton dissociation constants of pyrrolic nitrogens, and *in vivo* and *in vitro* superoxide dismuting activities of manganese(III) and iron(III) water-soluble prophyrins. Inorg Chem 1999;38:4011–22.
27. Katsumoto T, Higaki K, Phno K, Onodera K. Cell-cycle dependent biosynthesis and localization of p53 protein in untransformed human cells. Biol Cell 1995;84:167–73.

# p53 Translocation to Mitochondria Precedes Its Nuclear Translocation and Targets Mitochondrial Oxidative Defense Protein-Manganese Superoxide Dismutase

Yunfeng Zhao, Luksana Chaiswing, Joyce M. Velez, et al.

*Cancer Res* 2005;65:3745-3750.